Iron Oxide-Coated GAC Adsorbents: Diffusion-Controlled Sorption of Selenite

ARTICLE *in* INDUSTRIAL & ENGINEERING CHEMISTRY RESEARCH · JANUARY 2011

Impact Factor: 2.59 · DOI: 10.1021/ie100932r

4 AUTHORS, INCLUDING:

Dong Yan
University of Louisiana at Lafayette
4 PUBLICATIONS **3** CITATIONS
SEE PROFILE

Daniel Dianchen Gang
University of Louisiana at Lafayette
59 PUBLICATIONS **594** CITATIONS
SEE PROFILE

I&EC research
Industrial & Engineering Chemistry Research

ARTICLE

pubs.acs.org/IECR

Iron Oxide-Coated GAC Adsorbents: Diffusion-Controlled Sorption of Selenite

Dong Yan,[†] Daniel Dianchen Gang,[*,†] Ning Zhang,[‡] and LianShin Lin[‡]

[†]Department of Civil Engineering, University of Louisiana at Lafayette, P.O. Box 42291, Lafayette, Louisiana 70504, United States

[‡]Department of Civil and Environmental Engineering, College of Engineering and Mineral Resources, West Virginia University, Morgantown, West Virginia 26506, United States

ABSTRACT: Iron oxide-impregnated granular activated carbon has been proven to be successful in removal of selenite (Se(IV)) from aqueous solution. However, the key application component of the mass transfer operations and diffusion coefficient has not been determined. In this study, a modified finite bath diffusion control model with changing initial Se(IV) concentrations was analytically derived, and a constant related to radius of the absorbent particle and the fractional attainment of adsorption was introduced into this model. Batch adsorption studies of Se(IV) onto Fe−GAC were conducted at three different initial concentrations ranged from 0.5 to 2.0 mg/L with loading rate from 0.21 to 0.80 g/L. Results confirmed that the modified model is applicable to both low initial concentration with low fractional attainment and high initial concentration with $\bar{X} > 0.5$, while the original model was only applicable for the low initial Se(IV) concentration. The observed sorption kinetics was consistent with the finite bath diffusion, with an average value of 2.9×10^{-4} cm^2/s for the product of the distribution coefficient and the effective diffusivity in the adsorption of Se(IV) on the iron oxide-coated granular activated carbon.

1. INTRODUCTION

In recent years, the increasing release of toxic metals from industrial waste into natural waters is causing considerable concern. One of the toxic metals is selenium (Se).[1,2] In the environment, selenium can exist in different oxidation states, elemental selenium (Se), selenite (SeO_3^{2-}), selenide (Se^{2-}), selenate (SeO_4^{2-}), and organic selenium.[3] Selenite and selenate are found to be thermodynamically stable, and they are the dominant species in aqueous systems.[4] Selenite is present in mildly oxidizing, neutral pH environments and typically humid regions. Selenate is the predominant form under ordinary alkaline and oxidized conditions.[5]

Selenium is one of the strongly enriched elements in coal, being present as an organoselenium compound, a chelate species, or as an adsorbed element.[6] Selenium can be a main contaminant in aquatic environments as a result of human activities, particularly those involving mining and burning of coal for power generation.[7] Coal mining activities can cause leaching of Se into surface waters, resulting in degraded water quality and bioaccumulation in the food chain, and lead to deterioration and deformity in fish and wildlife over time. High-profile examples of Se causing significant ecological damage have been reported.[8] Some of the researchers reviewed Se data from 9000 coal samples throughout the United States and found that the highest concentrations of selenium in coal were in Texas and Mississippi.[9] A variety of treatment technologies have been reported for selenium removal from contaminated waters. Examples include ion-exchange, reverse osmosis, nanofiltration, solar ponds, chemical reduction with iron, microalgal-bacterial treatment, zeolite, and Fe/Se coprecipitation. All of these approaches did well under optimal conditions,[10−13] but most of the systems are expensive or cannot be used for a flowing system, not suitable for mining wastewater treatment. Adsorption of Se by metal oxides such as iron oxides and aluminum oxide has been demonstrated as a promising method for selenium removal.[14−17] However, these adsorbents can be difficult to use in a continuous flow system due to their small particle size.

Due to the fact that iron oxide can form strong complexation with both selenium[14−17] and carboxyl and phenol groups in activated carbon,[18,19] a new granular adsorbent, iron oxide-coated granular activated carbon (Fe−GAC), was developed for Se removal in our previous studies. Iron-coated GAC (Fe−GAC) is expected to achieve higher removal efficiency due to its large specific surface area,[19,20] and it is expected that Fe−GAC is more applicable for continuous treatment processes due to its granular nature. Previous studies have demonstrated that Fe−GAC could successfully remove selenite (Se(IV)) from aqueous solution with an adsorption capacity of 2.50 mg-Se/g-adsorbent.[21,22]

Although iron oxide-impregnated granular activated carbon has been proven to be successful in removal of selenite (Se(IV)) from aqueous solution, the key application component of the mass transfer operations and diffusion coefficient, which is very important for predicting rates of mass transfer, has not been determined. The objective of this study is to confirm that the modified finite bath diffusion control model can be used to describe the Se(IV) adsorption kinetic behavior not only in low initial concentration with low fractional attainment but also in high initial concentration and then to obtain the key component of the mass transfer operation, diffusion coefficient.

Received: April 20, 2010
Accepted: December 19, 2010
Revised: December 14, 2010
Published: January 18, 2011

dx.doi.org/10.1021/ie100932r | *Ind. Eng. Chem. Res.* 2011, 50, 2214–2219

2. EXPERIMENTAL SECTION

2.1. Materials. All chemical solutions used in this study were prepared using deionized water and analytical-grade chemicals. Sodium selenite (Na_2SeO_3) was purchased from MP Biomedicals (Solon, OH). Ferrous chloride ($FeCl_2 \cdot 4H_2O$) and cyclohexane (spectrophotometric, 99%) were purchased from Fisher Scientific, Inc. (Rochester, NY). Sodium hypochlorite (NaClO, 13%), 2,3-diaminonaphthalene (97%), and hxdroxylamine hydrochloride (reagent) were obtained from ACROS Organics (Geel, Belgium)

A 1000 mg/L selenium(IV) stock solution was prepared by dissolving Na_2SeO_3 into 250 mL of deionized and distilled water containing 2.5 mL of concentrated hydrochloride acid. A working solution of 4 mg/L was prepared using the stock solution for the adsorption experiments.

2.2. Adsorbent Preparation and Characterization. The iron oxide-coated granular activated carbon (Fe−GAC) was prepared using Darco12 × 20 GAC, provided by Norit Americas Inc. (Marshall, TX). Sodium hypochlorite was used to oxidize ferrous to ferric iron mildly so that further precipitation of ferric oxide could take place on the GAC surface. A 0.1 M ferrous chloride solution was used for GAC coating. The solution was prepared by dissolving $FeCl_2 \cdot 4H_2O$ into deionized water, while nitrogen gas was being diffused into the solution to eliminate oxygen from the solution. A predetermined amount of GAC was then added to the solution, and the pH of the solution was adjusted to 4.3 ± 0.1. The mixture was gently stirred, while a predetermined volume of 13% NaClO solution was added drop by drop to oxidize the ferrous iron. The volume of NaClO added was determined to obtain a 2:0.5 (mol/mol) ratio of NaClO to $FeCl_2$. The Fe−GAC product was then washed with 200 mL of deionized water and dried at 80 °C for 1 h.[21] The iron oxide-coated granular activated carbon (Fe−GAC) was crushed so that it passed through 100-mesh sieves and was retained by 200-mesh sieves with an average diameter of 112 μm.

2.3. Batch Adsorption. All batch experiments were conducted in 250 mL conical flasks placed in the shaker (200 rpm, 25 °C). The conical flasks were periodically taken out, and the mixtures were filtered through a 0.45 μm membrane filter. The rate of Se(IV) adsorption onto Fe−GAC was measured as a function of time (from 0 to 48 h) for different initial concentrations and adsorbent loadings. The pH of the mixture solution was adjusted to 5 ± 0.3 to achieve the highest adsorption capacity based on previous pH effect studies.[21]

2.4. Selenium(IV) Measurement. A standard method was used for selenium(IV) concentration measurement with a detection limit of approximately 0.01 mg/L.[23] The method is based on a reaction of selenite ion with 2,3-diaminonaphthalene (DAN) that produced a brightly colored and strongly fluorescent piazselenol compound, which was extracted in cyclohexane and measured colorimetrically. The DAN solution was prepared by dissolving 200 mg of DAN in 200 mL of HCl (0.1 N), extracting three times with 25 mL of cyclohexane, and then discarding organic portions. The aqueous phase was filtered into an opaque container and then stored in a cool, dark place. Hydroxylamine−EDTA solution (HA−EDTA) was prepared by adding 4.5 g of Na_2EDTA and 12.5 g of hydroxylamine hydrochloride (NH_2OHHCl) into 500 mL of deionized water. For the colorimetric measurements, 2 mL of the HA−EDTA solution was added to a 50 mL test tube containing 10 mL of water sample. The pH of the mixture was adjusted to 1.5 ± 0.3 using HCl (5 N). The sample solution together with 5 mL of DAN solution were put into a covered water bath at 50 °C for 45 min for color formation. The sample solution was cooled and added with 2 mL of cyclohexane. The sample test tube was capped securely and shaken vigorously for 5 min. The sample was then allowed to stand for 5 min to allow separation of the organic layer from the aqueous solution, followed by aqueous phase removal using a disposable pipet. Organic layer was then analyzed by a UV−vis spectrophotometer (Varian, Cary 50) for selenium concentration at a wavelength of 480 nm. A control containing no adsorbent, treated the same way as the sample, was used to establish the initial Se(IV) concentration.

2.5. Model Development. *Finite-Bath Diffusion Model.* Molecular diffusion controls the rate of most mass transfer operations in micro- and nonporous media. Determination of the diffusion coefficient for the key component is very important for predicting rates of mass transfer and many other correlations. To find the diffusion constant, a modified finite-bath diffusion control model[24] was derived following the approach of Adams et al.[25] Assuming a linear change of concentration of adsorbate species across the shell from a value $\bar{C}$ on the surface of the adsorbent particle to zero at the surface of the inner core of the unconverted form of the iron oxide coating layer, one can write from Fick's first law

$$\bar{J} = \bar{D}\,\bar{C}/(\bar{r} - \bar{r}_i) \tag{1}$$

where $\bar{J}$ = flux per unit area in the coating layer, $\bar{r}_i$ = radius of the inner core comprising the unconverted coating layer on granular activated carbon, $\bar{r}$ = initial radius of the adsorbent particle, and $\bar{D}$ = diffusion coefficient of the adsorbate species within the converted form of the coating layer. The adsorbate concentration at the surface of the coating layer $\bar{C}$ can be related to the external concentration C by the expression[26]

$$\bar{C} = KC^{2-z} \tag{2}$$

where K and z are characteristic constants. Substituting eq 2 into eq 1 and expressing $\bar{J}$ (in moles per unit area of coating layer within the volume $\bar{V}$ of the adsorbent particles) in terms of the change in concentration of the volume V of the external solution, according to Gang et al.,[27] we can obtain

$$\frac{d(CV)}{dt} = \frac{-3\bar{V}\,\bar{D}KC^{2-z}}{\bar{r}(\bar{r} - \bar{r}_i)} \tag{3}$$

The fractional conversion of the coating layer ($\bar{X}$) can be represented by

$$\bar{X} = 1 - \frac{\bar{r}_i^3 - \bar{r}_s^3}{\bar{r}^3 - \bar{r}_s^3} \tag{4}$$

From eq 4, we obtain

$$\frac{\bar{r}_i}{\bar{r}} = \left[(1 - \bar{X}) + \bar{X}\left(\frac{\bar{r}_s}{\bar{r}}\right)^3\right]^{1/3} \tag{5}$$

where $\bar{r}_s$ = radius of the solid core of the adsorbent particle and the adsorbate concentration (C) is given by

$$C = C_0(1 - \omega\bar{X}) \tag{6}$$

where C_0 = initial adsorbate concentration in solution and ω = equivalent ratio, defined as the ratio of the total adsorption capacity of the adsorbent to the total adsorbate content of the

external solution. Substituting eq 6 into eq 3 yields

$$\frac{C_0 V\, \mathrm{d}(1-\omega\bar{X})}{\mathrm{d}t} = \frac{-3\bar{V}\,\bar{D}KC_0^{1-z}(1-\omega\bar{X})^{2-z}}{\bar{r}(\bar{r}-\bar{r}_i)} \quad (7)$$

By substituting eq 5 into eq 7, eq 8 was obtained

$$\frac{\mathrm{d}(1-\omega\bar{X})}{\mathrm{d}t} = \frac{-3\bar{V}\,\bar{D}KC_0^{1-z}(1-\omega\bar{X})^{2-z}}{V\bar{r}^2\left\{1-\left[(1-\bar{X})+\bar{X}\left(\frac{\bar{r}_s}{\bar{r}}\right)^3\right]^{1/3}\right\}} \quad (8)$$

To simplify the equation, Chanda and Rempel[28] ignored the term of $(\bar{r}_s/\bar{r})^3$ in the above eq 8 and take $\omega = 1$ for the special case when $(\bar{r}_s/\bar{r}) < 1$and for small values of $\bar{X}$. Thus, Chanda and Rempel's approximation was only applicable for low values of $\bar{X}$. However, $\bar{X}$ can be as high as 0.8−0.9 in practice, so the $\bar{X}(\bar{r}_s/\bar{r})^3$ term should not be neglected. In our study, a constant $\bar{X}_0$ was introduced into the equation to consider this effect. $\bar{X}_0$ is a constant related to $\bar{r}_s$ and the fractional attainment of equilibrium adsorption $\bar{X}$, which is defined as $\bar{X}_0 = \bar{X}(\bar{r}_s/\bar{r})^3$. On the basis of the definition of ω and high values of $\bar{X}$ conditions, ω can be approximately expressed as $(\bar{r}^3 - \bar{r}_s^3)/\bar{r}^3$, that is $\omega = [1 - (\bar{r}_s/\bar{r})^3]$. Thus, eq 8 becomes

$$\frac{\mathrm{d}(1-\omega\bar{X})}{\mathrm{d}t} = \frac{-3\bar{V}\,\bar{D}KC_0^{1-z}\left(1-\omega\bar{X}\right)^{2-z}}{V\bar{r}^2\left[1-\left(1-\omega\bar{X}\right)^{1/3}\right]} \quad (9)$$

According to the same simplification procedures as used by Chanda and Rempel,[27] eq 9 can be rewritten, with $U = 1 - \omega\bar{X}$, $\lambda = KC_0^{1-z}$, as

$$\frac{\mathrm{d}U}{\mathrm{d}t} = \frac{-3\bar{V}\,\bar{D}\lambda U^{2-z}}{V\bar{r}^2[1-U^{1/3}]} \quad (10)$$

$$\int \frac{1-U^{1/3}}{U^{2-z}}\,\mathrm{d}U = \int \frac{-3\bar{V}\,\bar{D}\lambda}{V\bar{r}^2}\,\mathrm{d}t + \mathrm{Const} \quad (11)$$

$$\frac{U^{z-1}}{1-z} - \frac{3U^{z-2/3}}{2-3z} = \left(\frac{3\bar{V}\,\bar{D}\lambda}{V\bar{r}^2}\right)t + \mathrm{Const} \quad (12)$$

when $t = 0$ and $U = 1$

$$\mathrm{Const} = (1-z)^{-1} - 3(2-3z)^{-1} \quad (13)$$

$$\frac{\left(1-\omega\bar{X}\right)^{z-1}}{1-z} - \frac{3\left(1-\omega\bar{X}\right)^{z-2/3}}{2-3z} = \left(\frac{3\bar{V}\,\bar{D}\lambda}{V\bar{r}^2}\right)t + \frac{1}{1-z} - \frac{3}{2-3z} \quad (14)$$

Expanding in Taylor series as the following and ignoring terms that are higher than quadratic in $\bar{X}$, we get

$$\frac{(1-\omega X)^{z-1}}{1-z} = \frac{1+(z-1)\left(-\omega\bar{X}\right)+\frac{(z-1)(z-2)}{2}\left(-\omega\bar{X}\right)^2}{1-z} \quad (15)$$

$$\frac{3\left(1-\omega\bar{X}\right)^{z-2/3}}{2-3z} = \frac{3}{2-3z}\left[1+\left(z-\frac{2}{3}\right)\left(-\omega\bar{X}\right)+\frac{\left(z-\frac{2}{3}\right)\left(z-\frac{5}{3}\right)}{2}\left(-\omega\bar{X}\right)^2\right] \quad (16)$$

We have the following approximations

$$\frac{1}{6}\left(\omega\bar{X}\right)^2 = \left(\frac{3\bar{V}\,\bar{D}\lambda}{V\bar{r}^2}\right)t \quad (17)$$

Since $\omega = [1-(\bar{r}_s/\bar{r})^3]$, according to Chanda and Rempel's[24] theory, the $(\bar{r}_s/\bar{r})^3$ term can be ignored and we obtained the original equation

$$\bar{X} = \left(\frac{18\bar{V}\,\bar{D}\lambda}{V\bar{r}^2}\right)^{1/2} t^{1/2} \quad (18)$$

In our study, $(\bar{r}_s/\bar{r})^3$ cannot be ignored. Since $\bar{X}_0 = \bar{X}(\bar{r}_s/\bar{r})^3$, $\omega = 1[-(\bar{r}_s/\bar{r})^3] = 1 - \bar{X}_0/\bar{X}$, so eq 17 becomes

$$\bar{X} = \left(\frac{18\bar{V}\,\bar{D}\lambda}{V\bar{r}^2}\right)^{1/2} t^{1/2} + \bar{X}_0 \quad (19)$$

Therefore, the plot of $\bar{X}$ verses $t^{1/2}$ should be linear, with constant $\bar{X}_0$ able to be determined from the intercept of the straight line. $\lambda\bar{D}$, the product of the distribution coefficient and the effective diffusivity, can be determined from the slope of the straight line.

According to Chanda and Rempel's[28] simplification, for $z \approx 1$, integration of eq 10 becomes

$$\int \left(\frac{1}{U} - \frac{1}{U^{2/3}}\right)\mathrm{d}U = -\frac{3\bar{V}\,\bar{D}\lambda}{V\bar{r}^2}t + \mathrm{Const} \quad (20)$$

$$\ln U - 3U^{1/3} = -\frac{3\bar{V}\,\bar{D}\lambda}{V\bar{r}^2}t + \mathrm{Const} \quad (21)$$

when $t = 0$ and $U = 1$, constant = −3. After U is substituted by $1 - \omega\bar{X}$ and ω is replaced by $1 - (\bar{r}_s/\bar{r})^3$ where $(\bar{r}_s/\bar{r})^3$ can be neglected, eq 21 becomes

$$\ln\left[1/\left(1-\bar{X}\right)\right] - 3\left[1-\left(1-\bar{X}\right)^{1/3}\right] = \frac{3\bar{V}\,\bar{D}\lambda}{V\bar{r}^2}t \quad (22)$$

In our study, $(\bar{r}_s/\bar{r})^3$ cannot be ignored and $\omega = [1 - (\bar{r}_s/\bar{r})^3] = 1 - \bar{X}_0/\bar{X}$, the modified equation is given as

$$\ln\left[1/\left(1-\bar{X}+\bar{X}_0\right)\right] - 3\left[1-\left(1-\bar{X}+\bar{X}_0\right)^{1/3}\right] = \frac{3\bar{V}\,\bar{D}\lambda}{V\bar{r}^2}t \quad (23)$$

Therefore, the plot of $\ln[1/(1 - \bar{X} + \bar{X}_0)] - 3[1 - (1 - \bar{X} + \bar{X}_0)^{1/3}]$ verses t should be linear, with constant $\lambda\bar{D}$ being determined from the slope of the straight line. Comparing with the original equations (eqs 18 and 22) in Chanda and Rempel's[28] study, a constant $\bar{X}_0$ was introduced into the modified model in

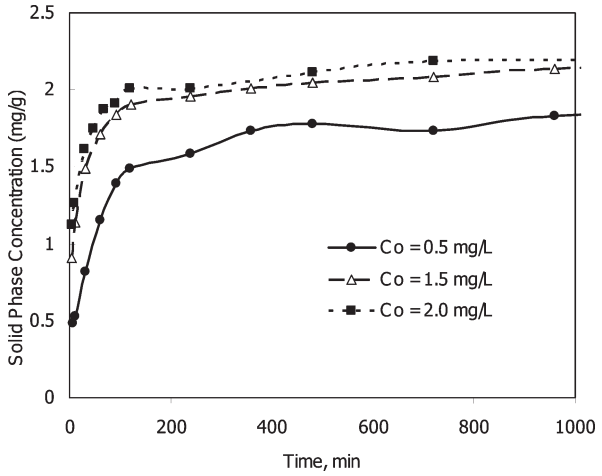

Figure 1. Adsorption kinetics of the Fe−GAC for Se(IV) at different initial concentrations: pH = 5 ± 0.3, temperature = 25 °C.

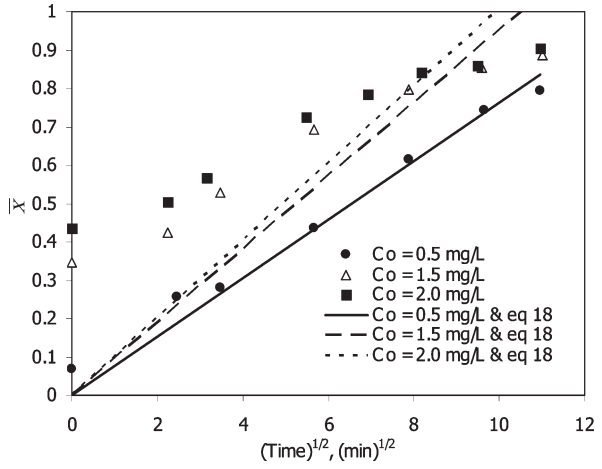

Figure 2. Test of eq 18 for the original model at different initial Se(IV) concentrations.

eqs 19 and 23. $\bar{X}_0$ is related to the radius of the absorbent particle and the fractional attainment of adsorption.

3. RESULT AND DISCUSSION

3.1. Adsorption Kinetics. The adsorbent loading for initial concentrations of 0.5, 1.5, and 2.0 mg/L was 0.21, 0.57, and 0.80 g/L, respectively. The experimental results are shown in Figure 1. The results indicated that the initial adsorption rate was fast, and the main adsorption was finished within about 6 h. Similar results were observed by others.[24] It was found that as the initial Se(IV) concentration increased from 0.5 to 1.5 mg/L, the solid-phase concentration increased from 1.875 to 2.15 mg/g, while the solid-phase concentration just changed a little, from 2.15 to 2.225 mg/g, when the initial concentration increased from 1.5 to 2.0 mg/L. This can be explained by the limitation of adsorption sites in the adsorbent. A similar result has been reported that the acceleration of adsorption capacity decreased due to occupation of adsorption sites by adsorbate.[29]

3.2. Finite-Bath Diffusion Model. The experimental data for the original eq 18 and modified eq 19 finite-bath diffusion models are plotted in Figures 2 and 3. The results show that both of the

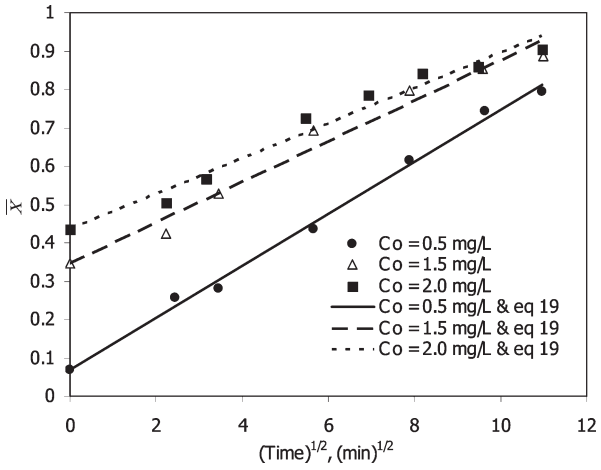

Figure 3. Test of eq 19 for the modified model at different initial Se(IV) concentrations.

Table 1. Values of $\lambda\bar{D}$ for Adsorption of Se(IV) on Fe−GAC at Different Concentrations for the Modified Model

		$\lambda\bar{D}$ (cm^2/s)			
C_0 (mg/L)	$\bar{X}_0$	eq *19*	R^2	eq *23*	R^2
0.5	0.0687	0.000272	0.99	0.000675	0.97
1.5	0.3453	0.000166	0.98	0.000284	0.99
2.0	0.4344	0.000127	0.97	0.000213	0.98

original and modified models are suitable for the lower initial Se(IV) concentration (0.5 mg/L), with a R^2 of 0.97 and 0.99, respectively. On the other hand, the original finite bath diffusion control model does not fit the high initial concentrations (1.5 and 2.0 mg/L) with R^2 of 0.76 and 0.63, respectively (Figure 2). It can be seen that the data fit the modified model very well with R^2 of more than 0.97 (Figure 3). The $\lambda\bar{D}$ values were calculated from the slopes of the modified model in Figure 3 and recorded in Table 1. The values of $\bar{X}_0$, the intercepts of the modified model lines, are listed in Table 1. From Figure 3 it can be seen that the $\bar{X}_0$ value increased as the initial concentration increased from 0.5 to 2.0 mg/L. This may due to the driving force increases as adsorbate concentration increases, which will increase the fractional attainment of Se(IV) adsorption. Because the adsorbent used for rate measurement was a mixture of particles of different shapes, but with a narrow size range, the average radius of the granular activated carbon (112 μm) was used for calculation of $\lambda\bar{D}$.

According to the original and modified finite-bath diffusion models, plots of $\ln[1/(1-\bar{X})] - 3[1-(1-\bar{X})^{1/3}]$ and $\ln[1/(1-\bar{X}+\bar{X}_0)] - 3[1-(1-\bar{X}+\bar{X}_0)^{1/3}]$ verses t should be linear. The data in Figure 1 are plotted in Figures 4 and 5 according to eqs 22 and 23. $\bar{X}_0$ obtained from eq 19 was used in eq 23. From Figures 4 and 5 it can be seen that both eqs 22 and 23 described the experimental data well with an average of $R^2 = 0.98$. The $\lambda\bar{D}$ values were calculated from the slope of the linear plots of Figure 5 and are recorded in Table 1. From Table 1 it can be seen that the $\lambda\bar{D}$ value decreased as the initial concentration increased from 0.5 to 2.0 mg/L. An average $\lambda\bar{D}$ value for the iron oxide-coated GAC adsorbent is 2.9×10^{-4} cm^2/s. Chanda and Rempel[28] found that the sorption of uranyl sulfate on PVP-coated silica gel correlated well with the original model. Their

dx.doi.org/10.1021/ie100932r |*Ind. Eng. Chem. Res.* 2011, 50, 2214–2219

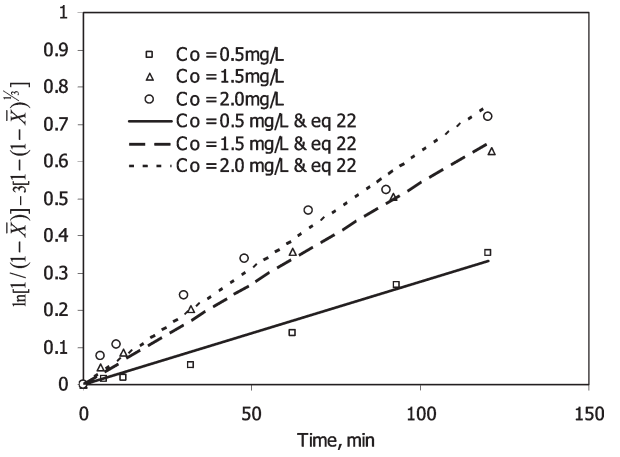

Figure 4. Test of eq 22 for the original model at different initial Se(IV) concentrations.

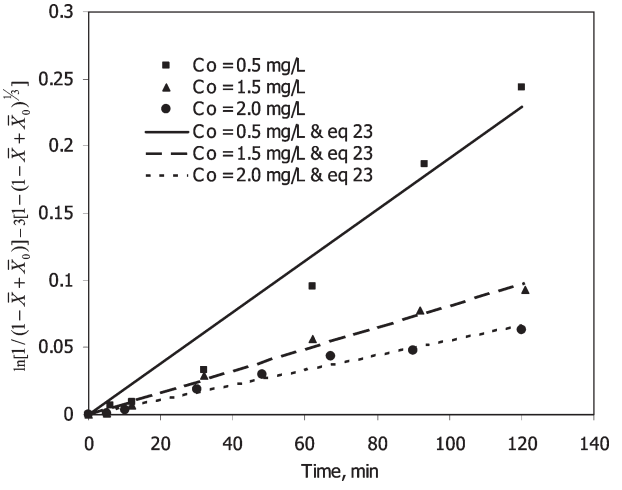

Figure 5. Test of eq 23 for the modified model at different initial Se(IV) concentrations.

reported $\lambda\overline{D}$ value was 5.4×10^{-6} cm^2/s. Gang et al.[24] got a $\lambda\overline{D}$ value of 4.1×10^{-6} cm^2/s for quaternized poly(4-vinylpyridine)-coated activated carbon. It can be seen that our value is much bigger than what they reported. One possible reason is that the iron oxide-coated layer is more loosely compared with the polymer layer reported by others. The main controlling mass transfer mechanism is pore surface diffusion, which was discussed in another study.[30] On the basis of above information, the modified finite-bath diffusion model fitted the experiments very well, with a diffusion coefficient of 2.9×10^{-4} cm^2/s.

AUTHOR INFORMATION

Corresponding Author

*Tel.:+1-337-482-5184. Fax: +1-337-482-6688. E-mail: Gang@louisiana.edu, dxy3848@louisiana.edu.

ACKNOWLEDGMENT

This work was supported by a US DOE grant (DE-FC26-02NT41607). The GAC sample was provided by Norit Americas Inc. (Marshall, TX).

NOMENCLATURE

C = adsorbate concentration in solution (mg/L)
$\overline{C}$ = adsorbate concentration at the particle surface (mg/L)
C_o = initial adsorbate concentration in solution (mg/L)
D = effective diffusivity in reacted layer (cm^2/s)
$\overline{r}_i$ = radius of the inner core (cm)
$\overline{r}$ = radius of the adsorbent particle (cm)
$\overline{r}_s$ = radius of the solid core of adsobent particle (cm)
J = flux per unit area in the iron oxide layer
K = characteristic constant $[(\text{mg/L})^{z-1}]$
t = time (min)
z = constant of nonuniformity
ω = equivalent ratio
$U = 1 - \omega X$
V = volume of external solution (L)
$\overline{V}$ = volume of adsorbent particle (L)
X = fractional attainment of equilibrium sorption
X_0 = fractional attainment constant
λ = distribution coefficient

REFERENCES

(1) Barbu, C.; Popescu, A.; Selisteanu, D.; Preda, A. Determination of toxic heavy metals present in Jiu river water using ICP-MS. *Asian J. Chem.* **2008**, *20* (3), 2037–2046.

(2) Ongeri, D.; Lalah, J. O.; Wandiga, S. O.; Schramm, K. W.; Michalke, B. Levels of toxic metals in multisectoral samples from winam gulf of Lake Victoria. *Bull. Environ. Contam. Toxicol.* **2009**, *82* (1), 64–69.

(3) James, A. I.; Kirk, G. S.; Ken, A. B. Selenium adsorption to aluminum-based water treatment residuals. *J. Colloid Interface Sci.* **2009**, *338*, 48–55.

(4) Ya, T. C.; Wen, H. K.; Tsan, Y. C.; Ming, K. W. Adsorption mechanism of selenate and selenite on the binary oxide systems. *Water Res.* **2009**, *43*, 4412–4420.

(5) Goh, K.; Lim, T. Geochemistry of inorganic arsenic and selenium in a tropical soil: effect of reaction time, pH, and competitive anions on arsenic and selenium adsorption. *Chemosphere* **2004**, *55*, 849–859.

(6) USEPA, Consumer Fact sheet on: Selenium, National Primary Drinking Water Regulations, www.epa.gov/safewater/dwh/c-ioc/selenium.

(7) Justin, M. C.; David, H. F.; David, B. B. Selenium bioaccumulation and maternal transfer in the mayfly centroptilum traingulifer in a life-cycle, periphyton-biofilm trophic assay. *J. Environ. Sci. Technol.* **2009**, *43*, 7952–7957.

(8) Muscatello, J. R.; Janz, D. M. Selenium accumulation in aquatic biota downstream of a uranium mining and milling operation. *Sci. Total Environ.* **2009**, *407* (4), 1318–1325.

(9) Coleman, L.; Bragg, L. J.; Finkelman, R. B. Distribution and mode of occurrence of selenium in US coals. *Environ. Geochem. Health* **1993**, *15* (4), 215–227.

(10) Nishimura, T.; Hashimoto, H.; Nakayama, M. Removal of selenium(VI) from aqueous solution with polyamine-type weakly basic ion exchange resin. *Sep. Sci. Technol.* **2007**, *42* (14), 3155–3167.

(11) Erosa, M. S. D.; Holl, W. H.; Horst, J. Sorption of selenium species onto weakly basic anion exchangers: I. Equilibrium studies. *React. Funct. Polym.* **2009**, *69* (8), 576–585.

(12) Shi, Y. S.; Wang, L.; Chen, Y.; Xu, D. W. Research on removing selenium from raw water by using Fe/Se co-precipitation system. *J. Water. Supply Res. T.* **2009**, *58* (1), 51–56.

(13) Yusof, A. M.; Idris, N. H.; Malek, N. A. N. N.; Wood, A. K. H. Use of granulated modified zeolite Y for the removal of inorganic arsenic and selenium species. *J. Radioanal. Nucl. Chem.* **2009**, *281* (2), 269–272.

(14) Peak, D.; Sparks, D. L. Mechanisms of selenate adsorption on iron oxides and hydroxides. *J. Environ. Sci. Technol.* **2002**, *36*, 1460–1466.

(15) Charlet, L.; Scheinost, A. C.; Tournassat, C.; Greneche, J. M.; Gehin, A.; Fernandez, M. A.; Coudert, S.; Tisserand, D.; Brendle, J. Electron transfer at the mineral/water interface: Selenium reduction by ferrous iron sorbed on clay. *Geochim. Cosmochim. Acta* **2007**, *71* (23), 5731–5749.

(16) Rovira, M.; Gimenez, J.; Martinez, M.; Martinez-Llado, X.; de Pablo, J.; Marti, V.; Duro, L. Sorption of selenium(IV) and selenium(VI) onto natural iron oxides: Goethite and hematite. *J. Hazard. Mater.* **2008**, *150* (2), 279–284.

(17) Su, T. Z.; Guan, X. H.; Gu, G. W.; Wang, J. M. Adsorption characteristics of As(V), Se(IV), and V(V) onto activated alumina: Effects of pH, surface loading, and ionic strength. *J. Colloid Interface Sci.* **2008**, *326* (2), 347–353.

(18) Pakula, M.; Biniak, S.; Swiatkowski, A. Chemical and electrochemical studies of interactions between iron (III) ions and an activated carbon surface. *Langmuir* **1998**, *14*, 3082–3089.

(19) Gu, Z.; Fang, J.; Deng, B. Preparation and evaluation of GAC-Based iron-containing adsorbents for arsenic removal. *Environ. Sci. Technol.* **2005**, *39*, 3833–3843.

(20) Vaughan, R. L., Jr.; Reed, B. E. Modeling As (V) removal by a iron oxide impregnated activated carbon using the surface complexation approach. *Water Res.* **2005**, *39*, 1005–1014.

(21) Zhang, N.; Lin, L.; Gang, D. Adsorptive selenite removal from water using iron-coated GAC adsorbents. *Water Res.* **2008**, *42*, 3809–3816.

(22) Zhang, N.; Gang, D.; Lin, L. Adsorptive removal of parts per million level Selenate using iron-coated GAC Adsorbents. *J. Environ. Eng.* **2010**, *136*, 1089–1095.

(23) Clesceri, L. S.; Greenberg, A. E.; Eaton, A. D. *Standard Methods for the Examination of Water and Wastewater, 3500-Se-C Colorimetric Method*, 20th ed.; American Public Health Association: Washington, DC, 1998.

(24) Gang, D.; Ravi, K.; Deng, B. Quaternized Poly (4-Vinylpyridine) Coated Activated Carbon: Diffusion Controlled Sorption of Chromium (VI). *J. Environ. Eng.* **2007**, *133* (8), 834–838.

(25) Adams, G.; Jones, P. M.; Millar, J. R. Kinetics of acid uptake by weak-base anion exchangers. *J. Am. Chem. Soc.* **1969**, 2543–2551.

(26) Glueckauf, E. A new approach to ion exchange polymers. *Proc. R. Soc. London, Ser. A.* **1962**, *268*, 350–370.

(27) Gang, D.; Banerji, S. K.; Clevenger, T. E. Modified poly (4-vinylpyridine) coated silica gel. Fast kinetics of diffusion controlled sorption of chromium (VI). *Ind. Eng. Chem. Res.* **2001**, *40* (4), 1200–1204.

(28) Chanda, M.; Rempel, G. L. Poly (4-vinylpyridine) gel coated on silica. High capacity and fast kinetics in uranyl sulfate recovery. *Ind. Eng. Chem. Res.* **1993**, *32* (4), 726–732.

(29) Liu, X. T.; Quan, X.; Bo, L. L.; Chen, S.; Zhao, Y. H.; Chang, M. Temperature measurement of GAC and decomposition of PCP loaded on GAC and GAC-supported copper catalyst in microwave irradiation. *Appl. Catal., A* **2004**, *264* (1), 53–58.

(30) Yan, D.; Gang, D.; Zhang, N.; Lin, L. Modeling selenite breakthrough with the pore surface diffusion model in iron coated granular activated carbon packed bed columns. *Proceedings of the 83rd Annual Water Environment Federation Technical Exhibition and Conference*, New Orleans, LA, 2010; Water Environmental Federation (WEF): Alexandria, VA; pp 5715−5727.